Preprints.org

Article

Not peer-reviewed version

MET Exon 14 Skipping and Novel Actionable Variants: Diagnostic and Therapeutic Implications in Latin American NSCLC patients.

Solange Rivas *, Romina V Sepulveda, Ignacio Tapia, Catalina Estay, Vicente Soto, Alejandro Blanco, Evelin Gonzáles, Ricardo Armisen *

Posted Date: 6 November 2024

doi: 10.20944/preprints202411.0367.v1

Keywords: non-small cell lung cancer; novel actionable variants; C-Met inhibitors; MET exon 14 skipping; next-generation sequencing

Preprints.org is a free multidisciplinary platform providing preprint service that is dedicated to making early versions of research outputs permanently available and citable. Preprints posted at Preprints.org appear in Web of Science, Crossref, Google Scholar, Scilit, Europe PMC.

Copyright: This open access article is published under a Creative Commons CC BY 4.0 license, which permit the free download, distribution, and reuse, provided that the author and preprint are cited in any reuse.

Preprints.org (www.preprints.org) | NOT PEER-REVIEWED | Posted: 6 November 2024 doi:10.20944/preprints202411.0367.v1

Disclaimer/Publisher's Note: The statements, opinions, and data contained in all publications are solely those of the individual author(s) and contributor(s) and not of MDPI and/or the editor(s). MDPI and/or the editor(s) disclaim responsibility for any injury to people or property resulting from any ideas, methods, instructions, or products referred to in the content.

Article

MET Exon 14 Skipping and Novel Actionable Variants: Diagnostic and Therapeutic Implications in Latin American NSCLC patients

Solange Rivas [1,*], Romina Sepúlveda [2], Ignacio Tapia [1], Catalina Estay [1], Vicente Soto [1], Alejandro Blanco [1], Evelin González-Feliú [1] and Ricardo Armisen [1,*]

[1] Centro de Genética y Genómica, Instituto de Ciencias e Innovación en Medicina, Facultad de Medicina Clínica Alemana Universidad del Desarrollo, Santiago 7550000, Chile
[2] Center for Bioinformatics and Integrative Biology, Facultad de Ciencias de la Vida, Universidad Andres Bello, Av. República 330, Santiago 8370146, Chile
* Correspondence: solange.rivas@udd.cl (S.R.); rarmisen@udd.cl (R.A.)

Abstract: Targeted therapy indications for actionable variants in non-small cell lung cancer (NSCLC) have primarily been studied in Caucasian populations, with limited data on Latin American patients. This study utilized a 52-gene next-generation sequencing (NGS) panel to analyze 1,560 tumor biopsies from NSCLC patients in Chile, Brazil, and Peru. RNA sequencing reads, and DNA coverage were correlated to improve the detection of the actionable MET exon 14 skipping variant (METex14). The pathogenicity of MET variants of uncertain significance (VUS) was assessed using bioinformatic methods based on their predicted driver potential. The effects of the predicted driver VUS T992I and H1094Y on MET signaling activation, proliferation, and migration were evaluated in HEK293T, BEAS-2B, and H1993 cell lines. Subsequently, MET inhibitors were tested in 2D and 3D cell cultures, and drug affinity was determined using 3D structure simulations. The prevalence of MET variants in the South American cohort was 8%, and RNA-based diagnosis detected 27% more cases of METex14 than DNA-based methods. Notably, 20% of METex14 cases with RNA reads below the detection threshold were confirmed by DNA analysis. The novel actionable T992I and H1094Y variants induced proliferation and migration through c-Met/Akt signaling. Both variants showed sensitivity to crizotinib and savolitinib, but the H1094Y variant exhibited reduced sensitivity to capmatinib. These findings highlight the importance of RNA-based METex14 diagnosis and reveal the drug sensitivity profiles of novel actionable MET variants from an understudied patient population.

Keywords: non-small cell lung cancer; novel actionable variants; C-Met inhibitors; MET exon 14 skipping; next-generation sequencing

1. Introduction

Lung cancer is the leading cause of cancer-related death worldwide, and non-small cell lung cancer (NSCLC) is the primary form of the disease, accounting for approximately 85% of cases. Lung cancer is often diagnosed at an advanced stage, making it challenging to provide curative therapy [1–3]. The treatments available for cancer patients before personalized medicine have shown a wide range of patient responses and relatively low survival [4]. In contrast, the implementation of tyrosine kinase inhibitors has decreased NSCLC mortality since 2013 [5]. Nowadays, the American Society of Clinical Oncology (ASCO) and the European Society for Medical Oncology (ESMO) recommend the sequencing of the actionable NSCLC genes, which means those genes with target therapy response, including *EGFR, ALK, ROS1, ERBB2, MET, MAP2K1, BRAF, KRAS*, *RET*, and NTRK1/2/3. The identification of actionable genes has contributed to the molecular characterization of NSCLC [6,7];

© 2024 by the author(s). Distributed under a Creative Commons CC BY license.

Preprints.org (www.preprints.org) | NOT PEER-REVIEWED | Posted: 6 November 2024 doi:10.20944/preprints202411.0367.v1

however, due to the limited implementation of personalized medicine, some populations, such as Latin American NSCLC patients, have been poorly characterized [6].

Among all NSCLC actionable genes, *MET* represents a critical oncogene that belongs to the transmembrane receptor tyrosine kinase family (RTK). The c-Met receptor is activated by the specific ligand hepatocyte growth factor (HGF) [7,8]. It induces the receptor dimerization, followed by the c-Met autophosphorylation of three tyrosine residues (Y1230, Y1234, and Y1235), and the consequent increase of the c-Met tyrosine kinase activity [9,10]. The canonical c-Met signaling pathways include RAS/MAPK, which promotes a proliferative and survival phenotype [11], and the PI3K/Akt/mTOR signaling, promoting survival, likewise a migratory phenotype [11,12].

The juxtamembrane domain encoded by exon 14 acts as a binding site for the c-Cbl E3 ubiquitin ligase for protein degradation [13]. However, the c-Met receptor is constitutively expressed when exon 14 is missing due to different mutational events [14]. The MET exon 14 skipping variant (METex14) is the only MET actionable variant recognized in NSCLC [15] and occurs in 2-3% of NSCLC patients, conferring clinical sensitivity to c-Met inhibitors such as crizotinib [16], capmatinib [17], tepotinib [18], and savolitinib [19]. These c-Met inhibitors are currently considered the first line of therapy or a subsequent therapy option in patients with advanced or metastatic NSCLC [20,21].

The METex14 variants affecting the splicing region represent a challenging diagnosis since the MET tumor's DNA sequencing has shown a low sensitivity [22,23]. Thus, sequencing of tumor RNA is the current gold standard diagnosis since it directly detects the fusion of exon 13 to exon 15, independent of the DNA variants that promote the exon 14 skipping [24]. The variants that induce METex14 represent a group of alterations at the region of the 3′ splice site in intron 13 or the 5′ end splice site of intron 14 involving donor or receptor sites and include single nucleotide variants (SNVs) as well as insertions and deletions (INDELs) of different lengths in the splicing regions at the beginning and the end of the exon 14 [15,25].

Diverse next-generation sequencing (NGS) based protocols have proposed a threshold number of RNA reads necessary to diagnose the METex14. For example, according to the user guide, the threshold for identifying METex14 by Oncomine® assay is at least 120 fusion reads [26]. However, a study suggested a threshold of 800 reads to mitigate potential difficulties in interpretation [27]. However, the clinically relevant question that remains unaddressed beyond the bioinformatic threshold is how many RNA reads (or other appropriate metrics) are necessary to achieve a successful therapeutic response to MET inhibitors? [27,28].

In addition to the canonical actionable METex14 variant, there is an increasing rate of conflicts reporting variants of unknown clinical significance (VUS) in the tumor profile of NSCLC patients, which are excluded from the target therapy prescription. However, with the advent of new bioinformatic algorithms, the reclassification of these VUS has benefited to assertively distinguish if those protein changes could be an actionable variant. For instance, the Cancer Genome Interpreter (CGI) platform's prediction algorithm helps identify driver variants that could potentially be treated with targeted therapies using BoostDM and OncodriveMut [29,30]. The Combined Annotation-Dependent Depletion (CADD) value is a pathogenicity predictor that integrates several genomic features and functional predictions [31]. The SIFT algorithm predicts whether an amino acid substitution is likely to affect protein function [32,33], and Polyphen-2 is another variant effect predictor that divided the analysis into three categories: benign, possibly damaging, and probably damaging to the protein function [34]. Johnson et al., recently demonstrated that at least 24% (106/438) of the VUS analyzed were oncogenic, and, most importantly, they identified 44% (204/438) as potentially actionable variants [35]. Certain *MET* mutagenic events, such as variants affecting the juxtamembrane or the tyrosine kinase domains, can transform the c-Met into an oncogenic protein. Thus, the study and identification of novel MET actionable variants that impact these domains is essential to broaden the prescription of already approved target drugs [13,36].

In this study, the analysis of the next-generation sequencing data of actionable genes from NSCLC South American patients evidenced 8% of MET variants versus 4% in the GENIE cohort. So, then we focused on the most prevalent MET variants, the METex14 (DNA versus RNA diagnosis), and the *in vitro* validation of two novel actionable variants categorized as VUS. Identifying actionable

Preprints.org (www.preprints.org) | NOT PEER-REVIEWED | Posted: 6 November 2024 doi:10.20944/preprints202411.0367.v1

and potentially actionable variants in underrepresented populations is essential since current, actionable variants have been identified primarily in Caucasian and non-Hispanic patients. Thus, identifying novel actionable variants in South American patients reduces disparities in diagnosing actionable variants, opening the benefits of available targeted therapies to a broader patient population.

2. Results

2.1. The Mutational Profiles of NSCLC Actionable Genes in South Americans Evidenced a High Prevalence of MET Exon 14 Skipping and Uncertain Significance MET Variants

The prevalence of protein-affecting variants (SNVs, indels, and gene fusions) in actionable NSCLC genes was estimated in 1,560 South American patients (NCT03220230)[37,38]). The clinical information and the DNA prevalence of variants were compared with a 100% Non-Spanish/Non-Hispanic Caucasian subset cohort of **18,857** NSCLC patients selected from GENIE [39] **(Table S1 and Figure 1).** *KRAS* was highly mutated in Caucasians, compared to the South American cohort (37% vs. 20%). The genes *ALK* (9% vs. 5%), *ERBB2* (8% vs. 4%), and *MET* (8% vs. 4%) were significantly more mutated in the South American NSCLC cohort **(Figure 1B).** The high prevalence of MET variants in our cohort and the slow regulatory approval process of MET inhibitors in the region prompted us to focus the analysis on this particular gene.

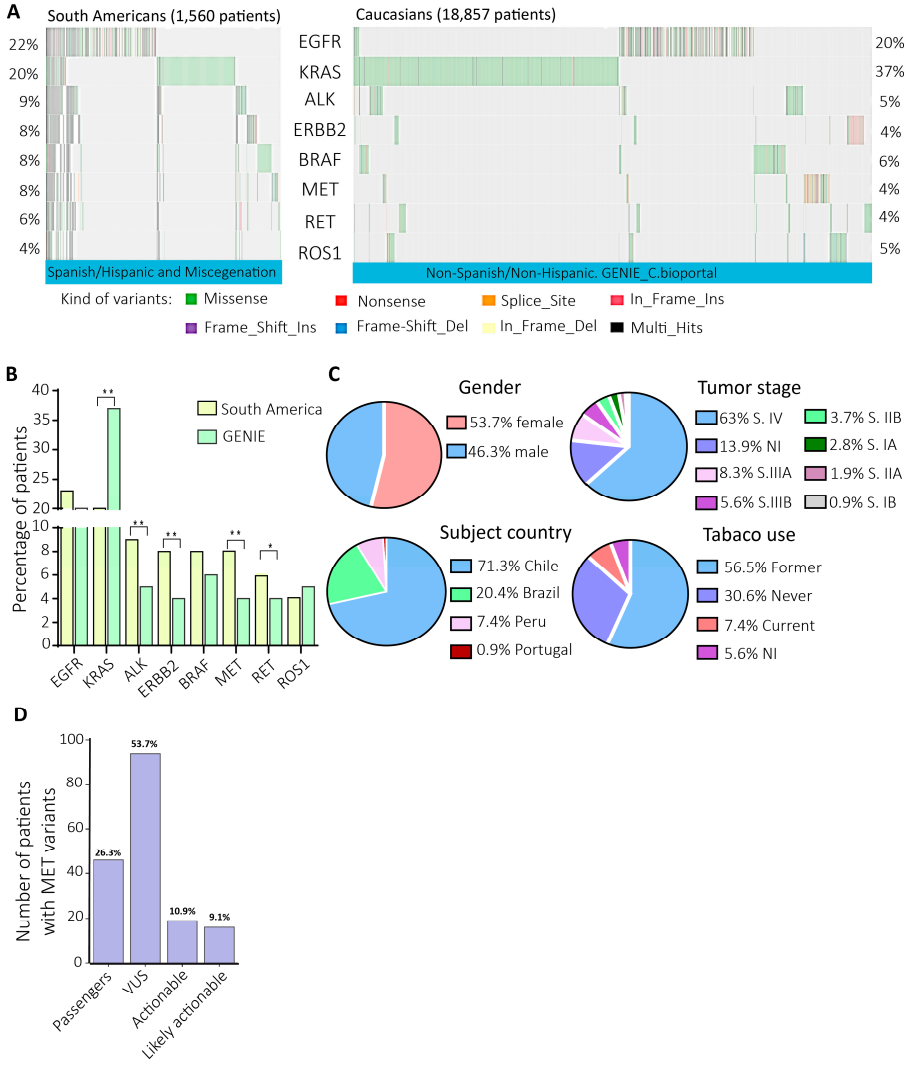

Figure 1. The mutational profiles of NSCLC actionable genes in South America evidenced a high prevalence of MET exon 14 skipping and uncertain significance MET variants. **A)** Each column of the oncoplots represents a patient and the rows show the prevalence of variants in the eight NSCLC

Preprints.org (www.preprints.org) | NOT PEER-REVIEWED | Posted: 6 November 2024 doi:10.20944/preprints202411.0367.v1

actionable genes. **B)** Variant prevalences´ comparison in eight actionable NSCLC genes. P-values= 0.008**. **C)** Gender, subject country, tumor stage, and tobacco use information of the patients with variants in the MET gene. **D)** MET variant categorization according to the clinical significance, the number, and the percentage of patients.

2.1.1. Clinical Characteristics of Patients with MET Variants

In the South American NSCLC cohort, 8% (123/1,560) of patients presented MET variants, 53.7% were women, 46.3% were men **(figure 1C)**, and 71.3% were from Chile, 20.4% were from Brazil and 7.4% from Peru **(Figure 1C).** The average age was 66 (**Figure S1A**). Almost all patients with MET variants evidenced one to three variants in any OFA genes (**Figure S1B**). At the diagnosis, 63% of the patients were at stage IV of the disease **(Figure 1C);** interestingly, 30.6% of patients with MET variants were never smokers, and 52.5% declared to be smoking former **(Figure 1C).**

The clinical significance categorization of the MET variants shows that 10.9% (19 patients) evidenced known actionable MET variants, followed by 9.1% of likely actionable variants (12 patients), which means diverse experts' panels highly recommend the use of MET inhibitors, but the regulatory agencies do not recognize these yet [40]. However, the VUS was the biggest category, with 53.7% (92 patients) of variants **(Figure 1D)**.

2.2. RNA and DNA MET Sequencing Analysis Evidenced Differences in Diagnosing the MET Exon 14 Skipping Variant

Nineteen DNA samples positive for METex14 variants evidenced SNVs and deletions in the region of the splice donor (SD) site, and interestingly, the analysis of these tumor biopsies (TBx) evidenced up to two SNVs at the splice region of *MET* (**Figure 2A, DNA regions affected in red**). In the RNA analysis, 72 patients showed between 20 to 67.000 RNA reads for the fusion of exons 13 and 15 **(Figure 2B)**. However, 48.6% (35/72) of patients were confirmed positive for the METex14 (> 120 RNA reads threshold), called the high RNA reads subgroup. Therefore, 37 patients with less than 120 RNA reads were categorized as undetermined (low RNA reads subgroup) following the Oncomine Focus Assay user guide [26], as depicted in **Figure 2C**.

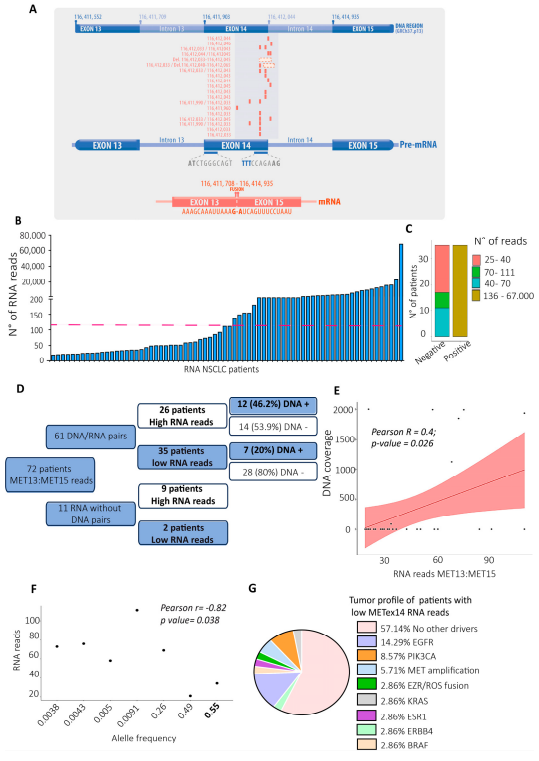

Figure 2. RNA and DNA MET sequencing analysis evidenced differences in diagnosing the MET exon 14 skipping variant. A) DNA regions of exons 13, 14, 15, and the introns 14 and 15 of the MET

Preprints.org (www.preprints.org) | NOT PEER-REVIEWED | Posted: 6 November 2024 doi:10.20944/preprints202411.0367.v1

gene (GRCh37.p13). Below are the DNA variants' locations that affect the coding sequence of exon 14 and the splicing donor region of the MET gene (variants located in red in rows) of each patient with a DNA variant in the SD region. **B)** The broad spectrum of RNA reads for the METex14 variant is shown in the x-axis. Each column represents a patient; the pink line defines the threshold (120 reads) for the positive MEtex14 diagnosis [26]. **C)** Number of patients categorized as negative and positive for METex14 according to the numbers of RNA reads. **D)** The conceptual map represents all TBx from NSCLC patients with a pair of RNA- and DNA-sequenced QC pass data. **E)** Pearson correlation between the RNA reads and the lectures from DNA. **F)** Pearson correlation analysis between the allele frequency of positive METex14 DNA variant (X-axis) with the number of RNA reads (Y-axis). **G)** Altered genes in the tumor profile of patients with low RNA reads for METex14.

Of patients with the RNA diagnosis of METex14, 53.9% were negative for METex14 in their DNA (**Figure 2D**), even in those with 3,170 – 9,487 and 12,301 RNA reads (**Table S2**). Here, the Pearson correlation between the DNA coverage and RNA reads was R= 0.45 with a P-value of 0.02, where the zero DNA lecture means no identification of the METex14 variant (**Figure S2A**). This moderate correlation indicates that in 45% of the cases, an increase in the RNA reads tends to increase the same unit in DNA lectures.

Regarding the 35 patients with less than 120 RNA reads, 20% (7 patients) showed variants in their DNAs located in the SD region at the 5′-exon 14 (**Figure 2A, the last 7 DNA regions in red, and Figure 2D)**. Here, the Pearson correlation between the low RNA reads subgroup and their DNA coverage was R= 0.38 and a p-value = 0.026 (**Figure 2E**), which indicates a moderate correlation in 38% of cases (**Figure S2A),** showing that the DNA and RNA MEtex14 diagnosis are moderately correlated independent of the number of RNA reads.

Nevertheless, the allele frequencies (AF) are unrelated to the number of RNA reads (**Figure 2F**). Some AF could suggest germinal variants (AF around 0.5); unfortunately, the information on germline variants for these patients is unavailable. Notably, 57.14% of these patients with low RNA reads did not report other actionable variants in their tumor profiles for any target therapy indication for solid tumors. However, this percentage could increase to 71.43%, considering that ESR1 (2.86%), ERBB4 (2.86%), and PIK3CA (8.57%) are not actionable genes in lung cancer (**Figure 2G**).

2.3. The MET T992I and H1094Y Are the Most Prevalent Predicted Driver Variants, Evidencing Biological Traits in Non-Tumor and NSCLC Cells Through the AKT Signaling Pathway

2.3.1. The VUS Represented 53.7% of all MET Variants (Figure 1C), so We Sought Those That Could Predict Actionability

Considering c-Met functional domains, we choose the variants that impacted the JM and the TK domains (**Figure 3A**). To gather more information about the driver statement of these VUS, bioinformatic algorithms such as SIFT, mutation taster, and PolyPhen-2 were chosen to predict the potential effect of the variants in the protein function, which is informed as tolerated (T), neutral (N) and deleterious variant (D). In addition, the CADD assigned a score between 0 – 40, whereas a high pathogenicity potential core is over 25. Finally, CGI predicted if those VUS were passengers, known or predicted actionable variants. Intriguing, most of the variants in these domains were predicted as potential drivers, as shown in the heatmap (**Figure 3B, Table S3**). Finally, the two most prevalent VUS predicted drivers were the T992I, which affected the JM domain (11 patients), and the H1094Y, which affected the TK domain (6 patients). Besides, 41.2% of these 17 patients with T992I and H1094Y did not report another driver or actionable variants in their tumor mutational profile **(Figure S3**), a percentage that reached 57.1% of patients without therapy option considering PIK3CA (14.3%), IDH2 (7.1%) and MTOR (7.1%) are not actionable lung cancer genes.

Preprints.org (www.preprints.org) | NOT PEER-REVIEWED | Posted: 6 November 2024 doi:10.20944/preprints202411.0367.v1

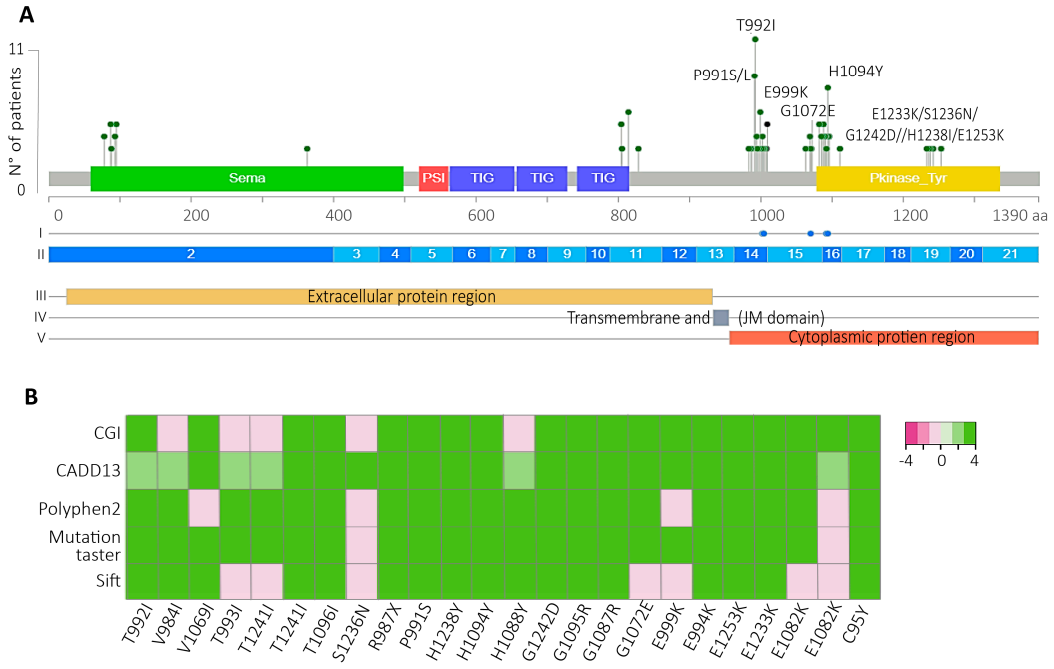

Figure 3. T992I and H1094Y were the most prevalent and bioinformatically predicted drivers and actionable. A) All VUS were localized in the Met protein domains. The green, red, blue, and yellow rectangles represent the location of the Sema, PSI, TIG, and kinase protein domains, respectively. Above the lolliplot, (I) Dots blue represent sensitive regions to target therapies, according to Oncokb. (II) The exons are represented in blue and light blue boxes. (III-IV-V) subcellular location of the mature protein. **B)** Driver prediction of the VUS located at the JM and TK domains (x-axis) by the bioinformatic algorithms CGI, Cadd13, polyphen2, mutation taster, and sift. Light pink and white color evidence predicted passengers and tolerated variants; green colors refer to those variants' predicted drivers.

2.3.2. The VUS Predicted Driver Induced a Migratory Phenotype and the Survival of Proliferative Cells in NSCLC and Non-Tumor Cells, Respectively

The expression of the T992I, H1094Y, and METex14 variants in non-tumor HEK293T cells, NSCLC H1993 cells, and BEAS-2B was confirmed by western blots (**Figure 4 A-D** and **S4)**. HEK293T cells expressing METex14, T992I, and H1094Y increased survival in response to 24 h of HGF incubation, where the T992I evidenced a significant survival regarding METex14 and the H1094Y variants. Besides, the NSCLC H1993 cells did not evidence a change in response to HGF in any experimental condition (**Figure 4E**). However, these cells showed a high migration rate, estimated through the wound closure percentage in response to HGF (**Figure 4 F-G**).

Preprints.org (www.preprints.org) | NOT PEER-REVIEWED | Posted: 6 November 2024 doi:10.20944/preprints202411.0367.v1

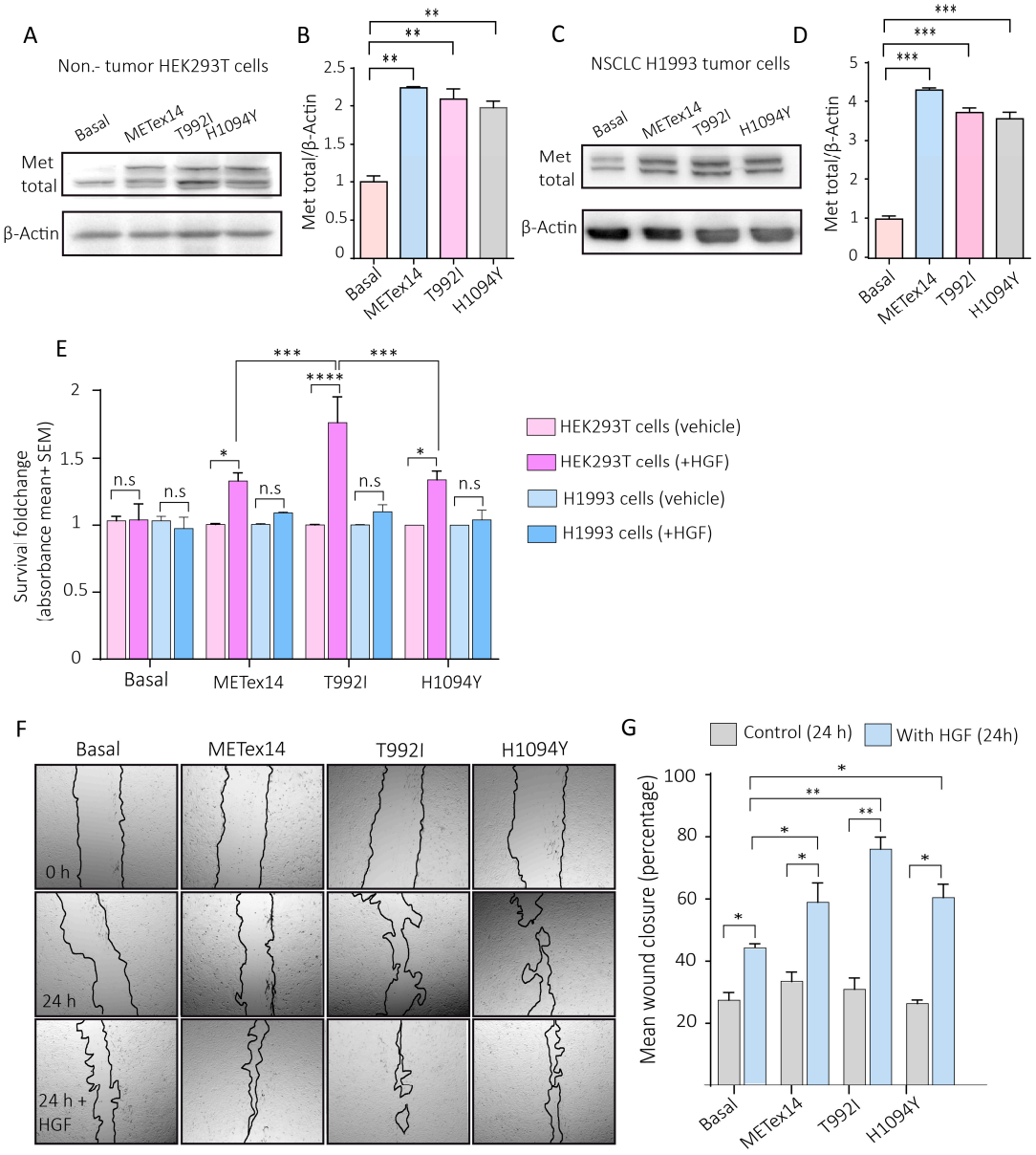

Figure 4. The VUS predicted driver T992I and H1094Y promote survival of proliferative non-tumor cells and migration in tumor cells. A) Representative western blots of total Met and β-actin expression evaluated for the H1993 GFP (basal), METex14, T992I, and H1094Y cells. B) Densitometry levels of total Met/β-actin normalized (+SEM). The graph represents the normalized average from 3 independent experiments ±SEM. C) Representative western blots of total Met and β-actin expression evaluated for the HEK293T GFP (basal), METex14, T992I, and H1094Y cells. D) Densitometry levels of total Met/β-actin normalized (+SEM). The graph represents the normalized average from 3 independent experiments ±SEM. E) The absorbance averages of HEK293T and H1993 cells expressing GFP, METex14, T992I, and H1094Y, the cells incubated with and without HGF. F) Representative images of the wound healing assay at 0 and 24 hours of H1993 cells expressing METex14, T992I, and H1094Y treated with and without HGF. G) The wound closure percentage was calculated for each experimental condition. Finally, three independent experiments averaging ±SEM are shown. Two-way ANOVA with Tukey correction was applied, and the p-values were adjusted for multiple comparisons *p<0.05; **p<0.01; ***p<0.001; n.s., non-significant.

Preprints.org (www.preprints.org) | NOT PEER-REVIEWED | Posted: 6 November 2024 doi:10.20944/preprints202411.0367.v1

2.3.3. The VUS T992I and the H1094Y Increase Met Autophosphorylation and the Downstream Akt Activation

To know if the variants induced migration and survival through the c-Met activation, the protein extract of the Hek293T cells expressing Metex14, T992I, and H1094Y were evaluated through western blot, evidencing a high level of c-Met activating phosphorylation (Metp), and the activating phosphorylation of Akt (Aktp) (**Figure 5 A-C**). However, the H1993 cells expressing METex14, T992I, and H1094Y did not show changes in Metp; nevertheless, the levels of the activating phosphorylation on Akt were significantly higher in the METexon14, T992I, and H1094Y conditions (**Figure 5 D-F**). Still, we noticed high levels of Metp/β-actin in all experimental conditions (**Figure 5G**), evidencing a proportional increase of the Metp regarding the Met total expression (**Figure 5H**). In addition, the bronchial-alveolar cells BEAS-2B also showed an increased Metp and Aktp in the METex14, T992I, and H1094Y compared with the basal expression **(Figure S5 A-D**).

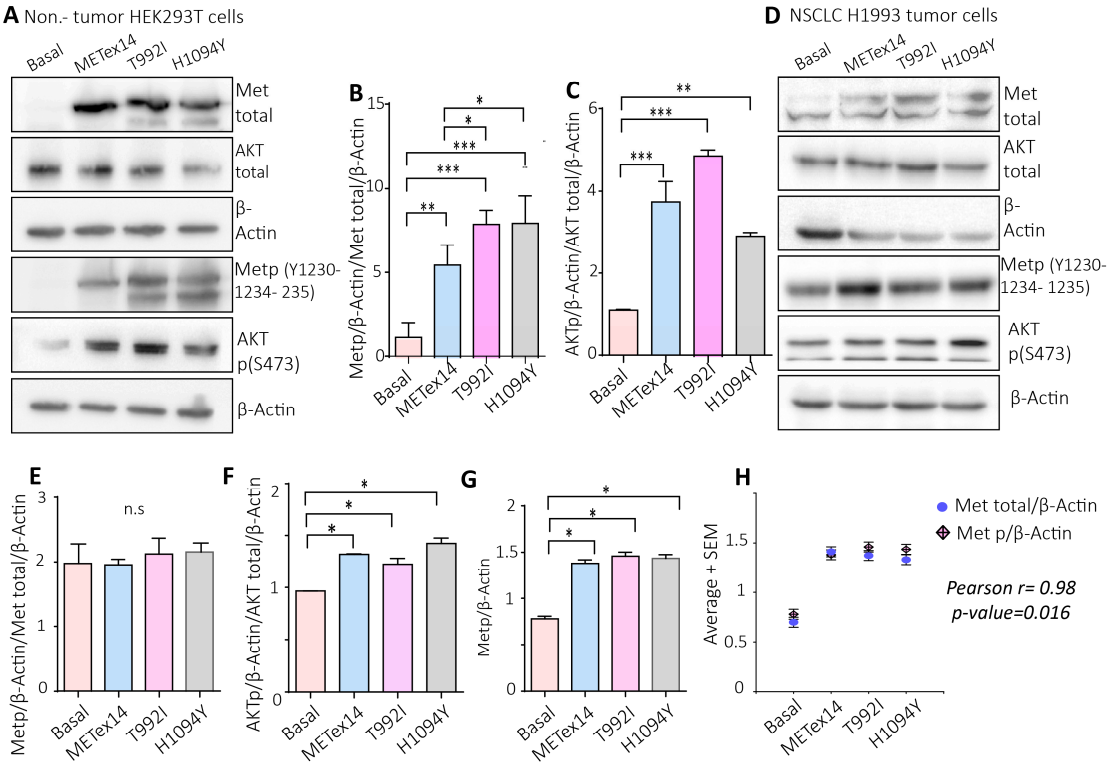

Figure 5. The VUS predicted driver T992I and the H1094Y increase the Met activating phosphorylation and the downstream Akt signaling pathway. A) Representative western blot images of total Met, total Akt , β-actin, Met p(Y1230-1234-1235), and Akt p(S473) proteins expression of HEK293T cells. B-C) Densitometry levels of Met phosphorylation, Akt phosphorylation, and β-actin were normalized relative to the total Met and Akt. D) Representative western blots of total Met , total Akt , β-actin, Met p(Y1230-1234-1235), and Akt p(S473) protein expression of H1993 cells. E-F) Densitometry levels of Met phosphorylation, Akt phosphorylation, and β-actin normalized relative to the total Met and Akt for H1993 cells. Graphs represent the normalized average from 3 independent experiments ±SEM. G) Densitometry levels of Metp relative to β-actin levels. H) Pearson correlation between the Metp and Met total relative to β-actin levels. One-way ANOVA with Tukey correction was applied, and the p-values were adjusted for multiple comparisons *p<0.05; **p<0.01; ***p<0.001; n.s., non-significant.

Preprints.org (www.preprints.org) | NOT PEER-REVIEWED | Posted: 6 November 2024 doi:10.20944/preprints202411.0367.v1

2.4. VUS Predicted Driver Variants Are Sensitive to c-Met Inhibitors in 2D and 3D Cultures of Non-Tumor and Tumor Cells

C-Met inhibitors, such as crizotinib, capmatinib, and savolitinib, were approved based on clinical trials that included patients whose tumors harbored METex14. So, we estimated the half-maximal inhibitory concentration (IC_{50}) of crizotinib, capmatinib, and savolitinib in HEK293T cells expressing METex14 (**Figure S6**). Then, the cell response to the targeted treatments was evaluated, finding that all treatments decreased the viability of cells expressing the METex14, T992I, and H1094Y variants compared to their counterpart untreated or control cells **(Figure 6A)**. Furthermore, viability decreased in cells expressing the METex14 and T992I variants relative to their basal conditions treated with crizotinib, capmatinib, and savolitinib **(Table S4).** On the other hand, cells expressing the H1094Y showed a low sensitivity to capmatinib compared to crizotinib and savolitinib treatments. Indeed, the capmatinib treatment did not significantly reduce cell viability relative to the basal conditions **(Table S4).**

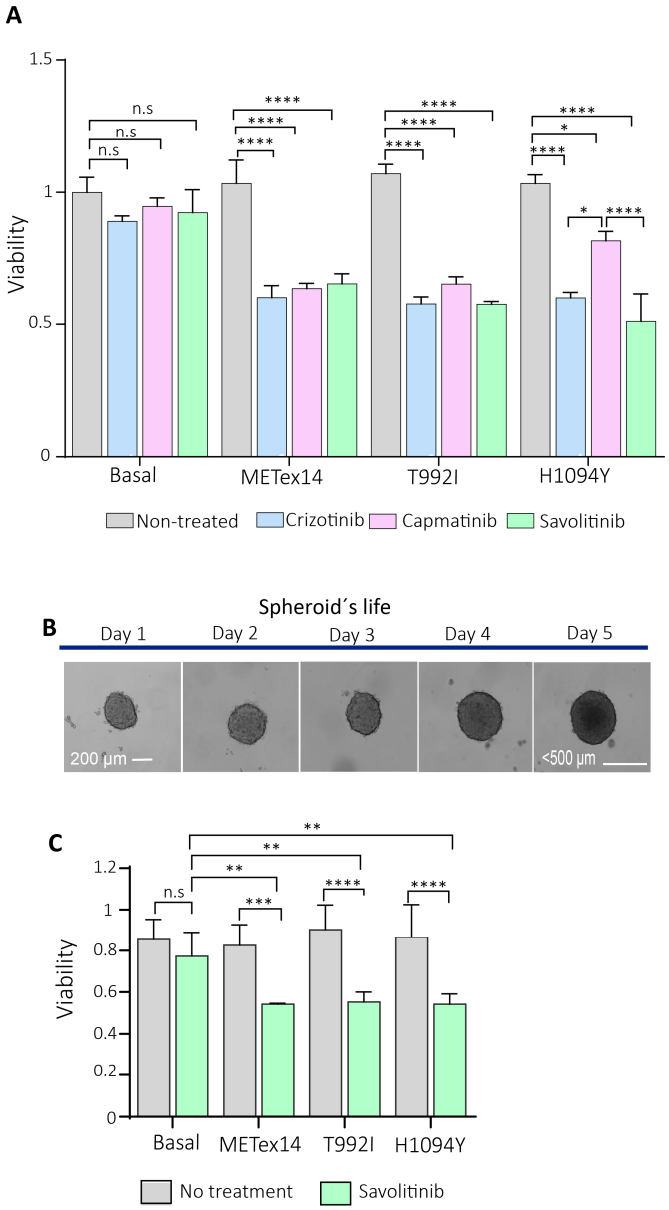

Figure 6. The 2D and 3D cell cultures expressing the Met-predicted driver variants were sensitive to c-Met inhibitors. A) 2,000 HEK293T expressing variants were seeded in 2D and incubated for 24 h with crizotinib, capatinib, and savolitinib. The absorbance was calculated from three independent experiments and normalized relative to the non-treatment culture cells. **B)**. Representative

Preprints.org (www.preprints.org) | NOT PEER-REVIEWED | Posted: 6 November 2024 doi:10.20944/preprints202411.0367.v1

microphotographs were captured with a Cytation3 imaging reader of the 3D H1993 cells (spheroid) each day of their life. At day 2 of spheroid formation (~200µm of sphere diameter), the drugs were incubated, and then the cells were released from the treatment until day 5. **C)** The spheroids were treated with savolitinib for 24h. Each experimental condition consisted of triplicates, averaged for each experimental condition. Finally, three independent experiments were averaged ±SEM. *p<0.05; **p<0.01; ***p<0.001.

2.4.1. Savolitinib Treatment in 3-Dimensional (3D) Culture Cells (Spheres)

As previously recommended, the spheroids lived until 120 h, not exceeding 500 microns in diameter [41] (**Figure 6B**). After 48 h of seeding, the spheres were treated with savolitinib for 24h. After 48h of drug release, the spheres expressing METex14, T992I, and H1094Y variants decreased the viability of proliferating cells in response to savolitinib treatment in comparison to the no treatment condition relative to the basal (**figure 6C**), strongly suggesting that the VUS T992I and H1094Y are actionable variants.

2.4.2. Analysis of Atomic Interactions of Active Protein Met WT, METex14, T992I, and H1094Y Variants with Savolitinib by Molecular Modeling, Docking, and Molecular Dynamics Simulations

The models revealed a significant region lacking secondary structure at the juxtamembrane domain, where the T992I variants are located. The secondary structure composition was analyzed along the trajectory, showing consistent levels of the alpha helix (23.8%) and beta-sheet (14%) in the Met WT system. These proportions were maintained in the presence of savolitinib across different systems, including WT:savolitinib, T992I:savolitinib, and H1094Y:savolitinib. However, Metex14 displayed variability in its secondary structure composition (30.4% alpha helix/11.7% beta sheet), suggesting potential changes in tertiary structure. The stability of savolitinib within the Met WT:savolitinib system is controlled by Y1159 (65% of the time) and M1169 (35% of the time) through a π-π interaction and hydrophobic contribution (**Figure S7**). Also, the interaction relies on the savolitinib pyrazolopyrimidine and D1030 (41% of the time) (**Figure 7A**) which explains the sensitivity. This is also observed in Met H1094Y:savolitinib system, where Y1094 is directly in contact with savolitinib **(Figure 7B)**. Concerning the T992I:savolitinib system, the average distance between the Cα T992I and the savolitinib is ~20Å, therefore, T992I is not a direct contact with savolitinib. The T992I:savolitinib induces a modification in the binding pocket where the H1094 loses its π-π interaction positioning at around 8Å from savolitinib (**Figure 7C**). Despite this, the savolitinib binding site remains due to D1164 (57% of the time) and M1169 (45% of the time). The METex14 system is composed of the juxtamembrane domain, which is not previously defined by structural studies, and significantly disrupts the structure of the Met tyrosine kinase, unable to establish the same stable binding pocket for savolitinib (**Figure 7D**). For more information, you can download the videos of the drug-protein interactions (Supplementary videos).

Preprints.org (www.preprints.org) | NOT PEER-REVIEWED | Posted: 6 November 2024 doi:10.20944/preprints202411.0367.v1

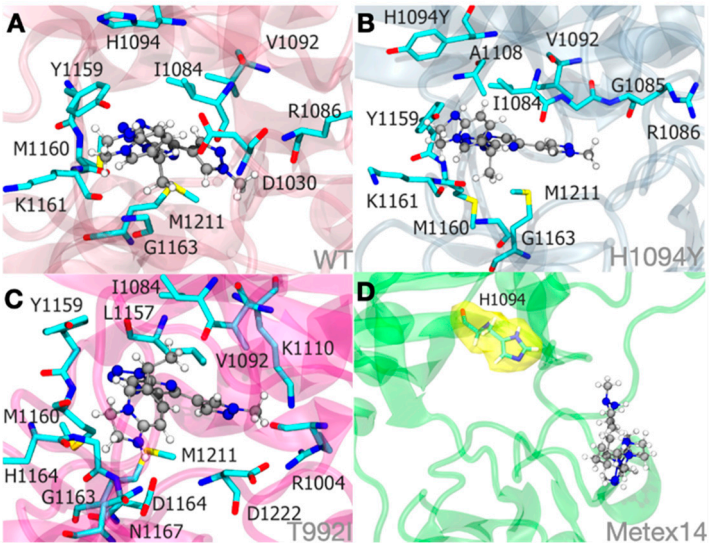

Figure 7. Molecular dynamics simulations illustrate the Savolitinib-MET protein system binding at an approximate mean distance of 3.0. The stability of the pyridazinone ring of savolitinib within the binding site of MET WT:SLB (A), MET H1094Y:SLB (B), and MET T992I:SLB (C) complexes is largely determined by hydrophobic interactions. Significantly, within the METex14:SLB complex (D), savolitinib is incapable of achieving a stable conformation due to substantial modifications in the initial loop that precedes the tyrosine kinase domain. Therefore, an unstable pocket site is produced. To clarify its proximity to savolitinib, the H1094 residue in the METex14:SLB complex (D) is highlighted in yellow in this context.

3. Discussion

Previously, 1,881 DNA and RNA from South American NSCLC patients' tumors were sequenced using the Oncomine focus assay [NCT03220230] [37]. Considering patients with DNA and RNA sequencing QC pass, the data analysis of 1,560 patients showed a prevalence of 8% of DNA MET variants, twice what is reported in the Caucasian/Non-Spanish/Hispanic patients from the GENIE cohort (**Figure 1B**) [39]**.** This finding is supported by data from the Caucasian and Asian NSCLC cohorts, which have evidenced a range from 0.9% to 4.0% of MET variants [42,43]. This high percentage of MET variants in the South American cohort was principally from Chile (71.3%), where MET inhibitors have not been approved yet [44]. On the other hand, Brazil has already approved the prescription of crizotinib, campatinib, and tepotinib [45], the same as in Argentina [46].

The METex14 variant was the most prevalent diagnosis, and at the RNA level, 72 TBx from NSCLC patients presented an extensive range of RNA reads for this variant (25 to 67.000 RNA reads). However, of these 72 patients, 35 had more than 120 RNA reads, which is the number required for diagnosing METex14, according to the user guide of the Oncomine Focus Assay [26]. Interestingly, 53.9% of these RNA diagnoses were negative at the DNA sequencing, evidencing the high sensitivity of the METex14 RNA diagnosis, as reported before [23].

In addition, 37/72 patients evidenced less than the 120 RNA reads for the METex14 detection; however, 20% of them evidenced pathogenic DNA variants in the splicing region of MET with diverse allele frequencies (**Figure 2A, G**). The splicing is a region often disrupted when a variant is present [47], confirming the possibility of false negatives METex14 diagnoses with less than 120 RNA reads. As the RNA sample from tumor biopsies is the gold standard for the METex14 diagnosis, in those cases with less than the RNA reads indicated in the user guide of the NGS kit, it would be necessary to suggest such as undetermined until the DNA sequencing or RT-PCR [48] brings some new evidence.

While how many METex14 RNA reads are indicative of a successful therapy with MET inhibitors continues to be unknown, it is essential to gather all the clinical and molecular evidence as

Preprints.org (www.preprints.org) | NOT PEER-REVIEWED | Posted: 6 November 2024 doi:10.20944/preprints202411.0367.v1

possible on those cases with low RNA reads whose tumor profiles did not evidence actionable nor driver variants, as the 57% of the patients with low RNA reads for METex14 analyzed here. Until now, the sole evidence about how many reads are required for a successful therapy with c-Met inhibitors is a case report informing the highest sensitivity of the OFA, which detected 46 reads for METex14 in an NSCLC patient without known actionable variants, who was previously treated with various chemotherapeutic agents without positive effects. The patient evidenced an immediate therapy response after administering tepotinib, a c-Met inhibitor [28].

Another interesting finding was the high percentage of VUS-predicted drivers impacted the JM and TK c-Met domains (**Figure 3A**), with the H1094Y and the T992I the most prevalent, which affected 14.41% of the patients with Met variants in the South American cohort. The H1094Y variant was first identified in renal cell carcinoma [49,50], and it has been detected as a resistance variant after glesatinib treatment in NSCLC positives for METex14 [51]. Also, this variant has been related to an oncogenic role in NSCLC conferring acquired resistance to EGFR-TKIs [52,53]. Although savolitinib has not been indicated by FDA yet, the combination of savolitinib plus osimertinib for NSCLC patients with MET-amplified or mutated with EGFR mutation-positive has been successful (NCT03778229) [54,55]. In NSCLC, the H1094Y variant has just been reported as a secondary resistance variant; however, the Chilean NSCLC patients studied here exhibited this variant before any therapy indication (**Figure 1E),** so here it is possible the H1094Y was the initial driver variant involved in the carcinogenesis in these patients.

The other novel actionable variant that evidenced the highest increase of c-Met activity through the proliferation and migration was the T992I, which has been previously reported as germinal in 4.5% of colon cancers, being considered an inherited risk factor for familial colorectal cancer [56], however, other studies described the T992I as a rare single nucleotide polymorphism not relevant to oncogenesis [57], however, this variant could be relevant in NSCLC progression, since here we found this variant reported the highest increase the Met activity, proliferation in non-tumor cells, and migration in tumor cells, in comparison to METex14 and H1094Y.

The study of these variants in South American patients also demonstrates the necessity of implementing the NGS for NSCLC patients in Chile as a universal health policy because until now, the clinical guides (Health Problem AUGE N°81) from Chile mention that this diagnosis and treatment are highly recommended, however, due to their high cost and lack of financing, constitute a barrier for patients [58]. Nonetheless, in the Chilean private health system, some hospitals offer sequencing analysis for the diagnosis of lung cancer.

As the already approved drugs such as savolitinib, capmatinib, and crizotinib evidenced a decrease in the viability of cells in culture cells, the next step would be to assess the efficacy of c-Met inhibitors in patients with these variants and without other known actionable, as recently tested in a patient with Met H1094Y [59]. An example of the NGS diagnosis and target therapy indication for patients with predicted actionable variants is the DRUP project (Drug Rediscovery Protocol), a nationwide Dutch program that considered patients with any advanced solid cancer to treat them with off-label precision drugs, considering the diagnosis the actionable and the bioinformatic predicted actionable variants as biomarkers for those patients excluded of target therapies indication due to the absence of known actionable variants [60]. So, to expand the use of already approved target drugs, validating c-MET inhibitors against novel actionable variants is a must.

4. Materials and Methods

South American NSCLC cohort. The cohort was selected from the study Characterization and Validation of Molecular Diagnostic Technologies for LC Patients from Chile, Brazil, and Peru (NCT03220230). The recruitment period was between July 2015 and October 2018, encompassing 37 health centers from three countries. A complete description of the study protocol has been provided previously [37,38].

Sequencing and quality control. Two to four Tbx FFPE sections of 5 μm with at least 5% tumor tissue were included. The RecoverAll extraction kit (Thermo Fisher Scientific) was used to isolate RNA and DNA. The Oncomine Focus Assay (OFA, Thermo Fisher Scientific) was used to prepare

Preprints.org (www.preprints.org) | NOT PEER-REVIEWED | Posted: 6 November 2024 doi:10.20944/preprints202411.0367.v1

libraries and sequenced in the Ion Personal Genome Machine System to perform the NGS. The QC metric thresholds were at least 240 median reads per amplicon, 60% of aligned reads for DNA libraries, 20,000 correctly mapped reads, and three out of five expression control amplicons detected for RNA.

Alignment and calling of variants. A minimum allele frequency of 5% (SNV) and 7% (Indel) was determined, and the minimum coverage that admits a variant was 10x (SNV and Indels). In addition, the minimum coverage of the variant location is 50x, with minimum variant scores in phred-scaled values set at 6 for SNV and 20 for Indels. All remaining reference/reference sites, variants with allelic frequency <5%, and observed alternative alleles <10 reads were removed from the DNA VCFs. For RNA VCFs, only fusions with more than 20 reads were maintained. Oncomine variants were selected as those located in positions within the predefined hotspot list of Oncomine Focus DNA Hotspots v1.4.

VUS-driver variants prediction. The clinical significance of the variants was obtained through the categorization made by Annovar [61], Cancer Genome Interpreter [30], and OncoKB[40]. Then, to annotate functional consequences of genetic variation of VUS, we used diverse predictor algorithms such as the Cancer Genome Interpreter (CGI) platform's prediction algorithm to identify driver variants that could potentially be treated with targeted therapies using BoostDM and OncodriveMut [29,30]. The Combined Annotation-Dependent Depletion (CADD) value is a pathogenicity predictor that integrates several genomic features and functional predictions [31]. The SIFT algorithm predicts whether an amino acid substitution will likely affect protein function [32,33]. Polyphen-2 is another variant effect predictor that divided the analysis into three categories: benign, possibly damaging, and probably damaging to the protein function [34], and Mutation Taster [62]. After obtaining all the algorithm's responses, the predicted driver variants were those confirmed as predicted drivers for all algorithms (Table S.3).

Culture cells. The H1993, HEK293T, and the BEAS-2B were maintained in RPMI 1640 (Gibco # 22400089) supplemented with 15% fetal bovine serum (SBF, Sigma #12103C), DMEM high glucose (Gibco # 12430054) supplemented with 10% SBF and the BEGM bronchial epithelial cell growth medium Bullet Kit (Lonza #CC-3170), respectively, all with 1% of penicillin/streptomycin (Thermo Fisher Scientific #15140122) in a CO_2 incubator at 37°C. Cells are routinely tested for mycoplasm.

Plasmids expression. The METex14 (pLV[Exp]-Puro-CMV (hMET[NM_001127500.3]*(delete exon 14)) (VB210712-1387jhm), T992I (pLV[Exp]-Puro-CMV (hMET[NM_000245.4]*(T992I)) (VB210720-1190man), H1094Y (pLV[Exp]-Puro-CMV (hMET[NM_000245.4]*(H1094Y)) (VB210720-1189kqp) were designed by Vector Builder, and the pLentiCMV MET GFP Puro (Addgene #37560) was acquired in Addgene. Dr. Marcelo Ezquer gently donated the transfection control GFP (pSIH1-H1-copGFP) vector. Lipofectamine 3000 was used in a proportion of 1:3 (DNA/lipofectamine) with the Opti-MEM™ I Reduced Serum Medium (Gibco # 31985070) as a vehicle, and after 48 hours, the cells were microphotographed in a Cytation3 and incubated with puromycin (1ug/ml) for 16 hours. The cells were allowed to expand for 2 to 5 days before carrying out the experiments.

Drugs. The Crizotinib (Cayman #12087), Capmatinib (Cayman, #INCB 28060), and Savolitinib (Cayman #33332) were used at 140nM, 130 nM and 40 nM, respectively, for 48 hours, and after a total of 72h, the MTS assay was carried out to measure the cell viability.

Western blot. The total proteins were extracted with lysis buffer 4x Laemmle buffer (#1610747, BIO-RAD), including a cocktail of protease and phosphatase inhibitors and 0.5 M dithiothreitol (DTT). Proteins were resolved by SDS-PAGE, transferred to the PDVF membranes, blocked with 5% bovine serum albumin (BSA, Sigma #A9418) in 0.1% TBS-Tween20, and blotted with specific antibodies MET total (Anti-Rabbit, #ab5662, ABCAM), Anti-Metp (phosphorylated on Y1230 + Y1234 + Y1235) antibody, #ab137654), anti-AKT (#4691, Thermo Fisher Scientific) and phosphorylated anti-AKT (#9271, Thermo Fisher Scientific) and β-actin (#A3853, Merck). Primary antibodies were prepared in a blocking solution, and membranes were incubated all night at 4 °C. Then, they were washed in TBS-Tween20 and further incubated with HRP-conjugated secondary antibodies. Samples were detected with EZ-ECL and visualized in an Amersham Imager 600 (GE Healthcare).

Preprints.org (www.preprints.org) | NOT PEER-REVIEWED | Posted: 6 November 2024 doi:10.20944/preprints202411.0367.v1

Survival of proliferative cells assay. The colorimetric assay CellTiter 96® AQueous One Solution Cell (Promega #G3582) was used to determine the number of viable cells in proliferation using 20 ul of tetrazolium compound for 4000-5000 cells [3-(4,5-dimethylthiazol-2-yl)-5-(3-carboxymethoxyphenyl)-2-(4-sulfophenyl)-2H-tetrazolium, inner salt; MTS in 200ul of final solution incubated for 2 h protected from the dark to then record the absorbance at 490 nm in the Citation3 absorbance reader. Then to graph the results, the absorbances were normalized.

Wound healing assay. Twenty-four hours after seeding the already transfected cells (empty GFP, METex14, T992I, and H1094Y) in 12-well plates with reduced fetal bovine serum, the cells were treated with and without 50 ng of recombinant human HGF (R&D #294-HG), and the wound was immediately made with a pipette tip of 200 µl. Using the Cytation3 microscope mode, ten measures were taken for each wound, and the percentage of wound closure was calculated relative to the wound distance average at time zero for each experimental condition.

Spheroid formation: First, the spheres were performed individually in a 96-well round plate previously precoated with the anti-adherent Poly(2-hydroxyethyl methacrylate) (pHEMA) stock solution at 120 mg/ml diluted in 95% ethanol PA, allowing it to homogenize while stirring overnight at room temperature, protected from light, to subsequently, on the same day of use, create a working solution at a concentration of 5 mg/ml to incubate the 96-well round bottom plates. Then, the plates were incubated for 72 hours at 37°C or until the polymer was dry and translucent. Once dry, the plates were sterilized under UV light for 15 minutes and sealed with Parafilm to keep them at 4°C upside down. Next, once stabilized at room temperature, the seeding of 3,500 H1993 cells was chosen, which was the optimal number of cells so that the sphere did not exceed 500 µm in diameter using the cell homogenate technique with 100 µl of RPMI. The spheroid's size was measured with the Cytation3 software, taking the mean of three different diameters per sphere**.** The 3 independent experiments were performed using five spheres (15 spheres in total) for each experimental condition.

Statistical analysis: All statistical analyses were performed with at least three independent experiments. Statistical differences between the two conditions were assessed with a non-parametric t-test (Mann–Whitney correction). Comparisons between more than two conditions were analyzed with parametric one-way or two-way ANOVA (Tukey correction for multiple comparisons). Analyzes were performed with the GraphPad Prism 6 Software (San Diego, CA).

Molecular docking and simulations. Molecular docking was utilized to investigate the molecular foundation and potential biological effects of MET and Savolitinib (SLB). We chose to examine the segment of MET tyrosine kinase that is involved in drug interactions based on the documented functioning MET tyrosine kinase structures found in PDBid: 8AU3, 8AU5 (Grädler, Ulrich, et al. 2023). We developed five separate systems for this method: a) WT, b) WT:SLB, c) T992I:SLB, d) H1094Y:SLB, and e) METex14:SLB.

The protein structures for systems a), b), c), and d) were modeled in 3D by extracting amino acid residues 963 to 1345 from the entire MET sequence using AlphaFold [63]. These structures closely matched the secondary structure of PDBid: 8AU3 and 8AU5 [64]. We extracted the sequence segment corresponding to the original MET tyrosine kinase (1010-1345) in the case of Metexon14 and appended the preceding 70 amino acids to create a model of similar size. Savolitinib (SLB) structure was obtained from Drugbank (DB12048) and used as a ligand in the docking simulation process. The grid was positioned at residue H1094 to serve as a reference point for other medicines in experimental structures, resulting in a final size of 12 x 12 x 12 Å3. The Glide tool from the Schrodinger program was utilized for conducting docking simulations in the Extra Precision (XP) mode, as described by Friesner et al. in 2006. After identifying the possible starting location of SLB, the structure was evaluated to establish 5 molecular systems. The Protein Preparation Wizard in Schrödinger Suite 2023-4 was utilized to create the first configuration of the kinase enzyme structures. This involved incorporating hydrogen atoms, determining bond ordering, constructing rotamers, and assigning protonation states. Epik was utilized to predict the ionization and tautomeric states. The systems were hydrated using the TIP3P water model and subsequently balanced with a 0.15 mol/L NaCl solution, resulting in a final size of approximately 70 x 70 x 90Å3. An isothermal-isobaric ensemble was established at 300 K. Each system underwent production simulations lasting 500 nanoseconds.

Preprints.org (www.preprints.org) | NOT PEER-REVIEWED | Posted: 6 November 2024 doi:10.20944/preprints202411.0367.v1

Molecular dynamics simulations were performed utilizing the DESMOND software with the OPLS 2005 force field model.

Supplementary Materials: The following supporting information can be downloaded at the website of this paper posted on Preprints.org.

Author Contributions: Conceptualization, Solange Rivas and Ricardo Armisen. Data Curation, Evelin Gonzalez-Feliu and Alejandro Blanco. Formal analysis, Solange Rivas and Romina Sepúlveda. Visualization, Solange Rivas. Funding acquisition, Solange Rivas and Ricardo Armisen. Investigation, Solange Rivas. Project administration, Solange Rivas. Methodology, Solange Rivas, Catalina Estay, Vicente Soto, Romina Sepulveda and Ignacio Tapia. Software, Alejandro Blanco, Evelin Gonzalez-Feliu, and Ricardo Armisen. Supervision, Ricardo Armisen. Writing – Original Draft Preparation, Solange Rivas. Writing – Review & Editing, Ricardo Armisen and Solange Rivas.

Acknowledgments: We thank the patients who consented to provide tumor material and clinical data used in this study. Special acknowledgments to all the participants of the NIRVANA team [37] and the members of the Laboratorio de Genómica Funcional del Cáncer at the Centro de Genética y Genómica, Instituto de Ciencias e Innovación en Medicina, Facultad de Medicina Clínica Alemana Universidad del Desarrollo, Mr. Felipe Serrano for the illustration work (Biologo_Ilustrador at serranofeli@gmail.com) and Prof. Fernando Danilo Gonzalez Nilo for advice in structural biology data.

Funding: This research was funded by Postdoctoral Fondecyt grant number [3210455] and Anillo project grant number [ACT210079], financed by the National Research and Development Agency, ANID, Chile.

Institutional Review Board Statement: The study was conducted according to the guidelines of the Declaration of Helsinki and approved by the Institutional Ethics Committee at Facultad de Medicina Clinica Alemana Universidad del Desarrollo (protocol code 2021-26, April 2021).

Informed Consent Statement: Informed consent was obtained from all subjects involved in the study.

Data Availability Statement: Genie data is available through The AACR Project GENIE Consortium at cBioportal. The data supporting the findings of this study are available within the article and its supplementary materials.

Conflicts of Interest: R.A. received honoraria for conferences, advisory boards, and educational activities from Roche and Janssen, as well as grants and support for scientific research from Pfizer, Roche & Thermo Fischer Scientific. The founders had no role in the study's design; in the collection, analysis, or interpretation of data, the writing of the manuscript, or the decision to publish the results.

References

1. Hammerschmidt, S. and H. Wirtz, *Lung cancer: current diagnosis and treatment.* Dtsch Arztebl Int, 2009. **106**(49): p. 809-18; quiz 819-20. https://doi.org/10.3238/arztebl.2009.0809
2. Passiglia, F., et al., *Diagnosis and treatment of early and locally advanced non-small-cell lung cancer: The 2019 AIOM (Italian Association of Medical Oncology) clinical practice guidelines.* Crit Rev Oncol Hematol, 2020. **148**: p. 102862.https://doi.org/10.1016/j.critrevonc.2019.102862
3. Polanco, D., et al., *Prognostic value of symptoms at lung cancer diagnosis: a three-year observational study.* J Thorac Dis, 2021. **13**(3): p. 1485-1494. https://doi.org/10.21037/jtd-20-3075
4. Sharma, A., S. Jasrotia, and A. Kumar, *Effects of Chemotherapy on the Immune System: Implications for Cancer Treatment and Patient Outcomes.* Naunyn Schmiedebergs Arch Pharmacol, 2023. https://doi.org/10.1007/s00210-023-02781-2
5. Howlader, N., et al., *The Effect of Advances in Lung-Cancer Treatment on Population Mortality.* N Engl J Med, 2020. **383**(7): p. 640-649. https://doi.org/10.1056/NEJMoa1916623
6. Parra-Medina, R., et al., *Prevalence of oncogenic driver mutations in Hispanics/Latin patients with lung cancer. A systematic review and meta-analysis.* Lung Cancer, 2023. **185**: p. 107378. https://doi.org/10.1016/j.lungcan.2023.107378
7. Bottaro, D.P., et al., *Identification of the hepatocyte growth factor receptor as the c-met proto-oncogene product.* Science, 1991. **251**(4995): p. 802-4. https://doi.org/10.1126/science.1846706

Preprints.org (www.preprints.org) | NOT PEER-REVIEWED | Posted: 6 November 2024 doi:10.20944/preprints202411.0367.v1

8. Comoglio, P.M., *Structure, biosynthesis and biochemical properties of the HGF receptor in normal and malignant cells.* EXS, 1993. **65**: p. 131-65.
9. Faoro, L., et al., *MET receptor tyrosine kinase.* J Thorac Oncol, 2009. **4**(11 Suppl 3): p. S1064-5. https://doi.org/10.1097/01.JTO.0000361752.86918.09.
10. Zhao, Y., et al., *Lipopolysaccharide-induced phosphorylation of c-Met tyrosine residue 1003 regulates c-Met intracellular trafficking and lung epithelial barrier function.* Am J Physiol Lung Cell Mol Physiol, 2013. **305**(1): p. L56-63. https://doi.org/10.1152/ajplung.00417.2012
11. Paumelle, R., et al., *Hepatocyte growth factor/scatter factor activates the ETS1 transcription factor by a RAS-RAF-MEK-ERK signaling pathway.* Oncogene, 2002. **21**(15): p. 2309-19. https://doi.org/10.1038/sj.onc.1205297
12. Holt, R.U., et al., *Hepatocyte growth factor promotes migration of human myeloma cells.* Haematologica, 2008. **93**(4): p. 619-22. https://doi.org/10.3324/haematol.11867
13. Onozato, R., et al., *Activation of MET by gene amplification or by splice mutations deleting the juxtamembrane domain in primary resected lung cancers.* J Thorac Oncol, 2009. **4**(1): p. 5-11. https://doi.org/10.1097/JTO.0b013e3181913e0e.
14. Kong-Beltran, M., et al., *Somatic mutations lead to an oncogenic deletion of met in lung cancer.* Cancer Res, 2006. **66**(1): p. 283-9. https://doi.org/10.1158/0008-5472.CAN-05-2749
15. Frampton, G.M., et al., *Activation of MET via diverse exon 14 splicing alterations occurs in multiple tumor types and confers clinical sensitivity to MET inhibitors.* Cancer Discov, 2015. **5**(8): p. 850-9. https://doi.org/10.1158/2159-8290.CD-15-0285
16. Drilon, A., et al., *Antitumor activity of crizotinib in lung cancers harboring a MET exon 14 alteration.* Nat Med, 2020. **26**(1): p. 47-51. https://doi.org/10.1038/s41591-019-0716-8
17. Wolf, J., et al., *Capmatinib in MET Exon 14-Mutated or MET-Amplified Non-Small-Cell Lung Cancer.* N Engl J Med, 2020. **383**(10): p. 944-957. https://doi.org/10.1056/NEJMoa2002787
18. Paik, P.K., et al., *Tepotinib in Non-Small-Cell Lung Cancer with MET Exon 14 Skipping Mutations.* N Engl J Med, 2020. **383**(10): p. 931-943. https://doi.org/10.1056/NEJMoa2004407.
19. Lu, S., et al., *Once-daily savolitinib in Chinese patients with pulmonary sarcomatoid carcinomas and other non-small-cell lung cancers harbouring MET exon 14 skipping alterations: a multicentre, single-arm, open-label, phase 2 study.* Lancet Respir Med, 2021. **9**(10): p. 1154-1164. https://doi.org/10.1016/S2213-2600(21)00084-9
20. Desai, A. and S. Cuellar, *The Current Landscape for METex14 Skipping Mutations in Non-Small Cell Lung Cancer.* J Adv Pract Oncol, 2022. **13**(5): p. 539-544. https://doi.org/10.6004/jadpro.2022.13.5.8
21. Awad, M.M., et al., *MET Exon 14 Mutations in Non-Small-Cell Lung Cancer Are Associated With Advanced Age and Stage-Dependent MET Genomic Amplification and c-Met Overexpression.* J Clin Oncol, 2016. **34**(7): p. 721-30. https://doi.org/10.1200/JCO.2015.63.4600
22. Li, Y., et al., *Identification of MET exon14 skipping by targeted DNA- and RNA-based next-generation sequencing in pulmonary sarcomatoid carcinomas.* Lung Cancer, 2018. **122**: p. 113-119. https://doi.org/10.1016/j.lungcan.2018.06.001. https://doi.org/10.1016/j.jtho.2018.12.020
23. Davies, K.D., et al., *DNA-Based versus RNA-Based Detection of MET Exon 14 Skipping Events in Lung Cancer.* J Thorac Oncol, 2019. **14**(4): p. 737-741. https://doi.org/10.1016/j.jtho.2018.12.020
24. Poirot, B., et al., *MET Exon 14 Alterations and New Resistance Mutations to Tyrosine Kinase Inhibitors: Risk of Inadequate Detection with Current Amplicon-Based NGS Panels.* J Thorac Oncol, 2017. **12**(10): p. 1582-1587. https://doi.org/10.1016/j.jtho.2017.07.026
25. Drilon, A., *MET Exon 14 Alterations in Lung Cancer: Exon Skipping Extends Half-Life.* Clin Cancer Res, 2016. **22**(12): p. 2832-4. https://doi.org/10.1158/1078-0432.CCR-16-0229

Preprints.org (www.preprints.org) | NOT PEER-REVIEWED | Posted: 6 November 2024 doi:10.20944/preprints202411.0367.v1

26. Guide, I.T.U., *Ion Reporter™ Software 5.16 USER GUIDE.* 2020.https://assets.thermofisher.com/TFS-Assets/LSG/manuals/MAN0019148_IonReporter_5_16_UG.pdf (acceded 24.09.2024)
27. Teishikata, T., et al., *An Alert to Possible False Positives With a Commercial Assay for MET Exon 14 Skipping.* J Thorac Oncol, 2021. **16**(12): p. 2133-2138. https://doi.org/10.1016/j.jtho.2021.07.028
28. Onodera, Y., et al., *Successful tepotinib treatment of adenocarcinoma with MET exon 14 skipping and discordant results between Oncomine Dx target test and ArcherMET: A case report.* Mol Clin Oncol, 2023. **18**(6): p. 49. https://doi.org/10.3892/mco.2023.2645
29. Muinos, F., et al., *In silico saturation mutagenesis of cancer genes.* Nature, 2021. **596**(7872): p. 428-432. https://doi.org/10.1038/s41586-021-03771-1
30. Tamborero, D., et al., *Cancer Genome Interpreter annotates the biological and clinical relevance of tumor alterations.* Genome Med, 2018. **10**(1): p. 25. https://doi.org/10.1186/s13073-018-0531-8
31. Rentzsch, P., et al., *CADD: predicting the deleteriousness of variants throughout the human genome.* Nucleic Acids Res, 2019. **47**(D1): p. D886-D894.https://doi.org/10.1093/nar/gky1016
32. Ng, P.C. and S. Henikoff, *SIFT: Predicting amino acid changes that affect protein function.* Nucleic Acids Res, 2003. **31**(13): p. 3812-4. https://doi.org/10.1093/nar/gkg509
33. Sim, N.L., et al., *SIFT web server: predicting effects of amino acid substitutions on proteins.* Nucleic Acids Res, 2012. **40**(Web Server issue): p. W452-7.https://doi.org/10.1093/nar/gks539
34. Adzhubei, I., D.M. Jordan, and S.R. Sunyaev, *Predicting functional effect of human missense mutations using PolyPhen-2.* Curr Protoc Hum Genet, 2013. **Chapter 7**: p. Unit7 20.https://doi.org/10.1002/0471142905.hg0720s76
35. Johnson, A., et al., *Actionability classification of variants of unknown significance correlates with functional effect.* NPJ Precis Oncol, 2023. **7**(1): p. 67.https://doi.org/10.1038/s41698-023-00420-w
36. Peschard, P., et al., *Mutation of the c-Cbl TKB domain binding site on the Met receptor tyrosine kinase converts it into a transforming protein.* Mol Cell, 2001. **8**(5): p. 995-1004.https://doi.org/10.1016/s1097-2765(01)00378-1
37. Sepúlveda-Hermosilla, G., et al., *Molecular characterization of non-small cell lung cancer tumors in Latin American patients from Brazil, Chile and Peru uncovers novel potentially driver mutations.* MedRxiv, 2020.https://doi.org/10.1101/2020.09.11.20171025
38. Sepulveda-Hermosilla, G., et al., *Concordance Analysis of ALK Gene Fusion Detection Methods in Patients with Non-Small-Cell Lung Cancer from Chile, Brazil, and Peru.* J Mol Diagn, 2021. **23**(9): p. 1127-1137.https://doi.org/10.1016/j.jmoldx.2021.05.018
39. de Bruijn, I., et al., *Analysis and Visualization of Longitudinal Genomic and Clinical Data from the AACR Project GENIE Biopharma Collaborative in cBioPortal.* Cancer Res, 2023. **83**(23): p. 3861-3867.https://doi.org/10.1158/0008-5472.CAN-23-0816.
40. Suehnholz, S.P., et al., *Quantifying the Expanding Landscape of Clinical Actionability for Patients with Cancer.* Cancer Discov, 2024. **14**(1): p. 49-65.https://doi.org/10.1158/2159-8290.CD-23-0467
41. Pinto, B., et al., *Three-Dimensional Spheroids as In Vitro Preclinical Models for Cancer Research.* Pharmaceutics, 2020. **12**(12).https://doi.org/10.3390/pharmaceutics12121186
42. Campbell, J.D., et al., *Distinct patterns of somatic genome alterations in lung adenocarcinomas and squamous cell carcinomas.* Nat Genet, 2016. **48**(6): p. 607-16. https://doi.org/10.1038/ng.3564
43. Xu, Z., et al., *Incidence and PD-L1 Expression of MET 14 Skipping in Chinese Population: A Non-Selective NSCLC Cohort Study Using RNA-Based Sequencing.* Onco Targets Ther, 2020. **13**: p. 6245-6253. https://doi.org/10.2147/OTT.S241231

Preprints.org (www.preprints.org) | NOT PEER-REVIEWED | Posted: 6 November 2024 doi:10.20944/preprints202411.0367.v1

44. Rivas, S. and R. Armisén, *El cáncer de pulmón de células no pequeñas en la era de la medicina de precisión.* Revista Médica Clínica Las Condes, 2022. **33**(1): p. 25-35.https://doi.org/10.1016/j.rmclc.2022.01.001
45. Anvisa, A.N.d.V.S.-. *Câmara de Regulação do Mercado de Medicamentos- CMED Secretaria Executiva*, n.h.s.a.f. Brazil, Editor. 2022: https://www.gov.br/anvisa/pt-br/assuntos/medicamentos/cmed/precos/arquivos/lista_conformidade_2022_03_v1x.pdf/view (acceded 24.09.2024).
46. MERCK. 2022; Available from: https://www.merckgroup.com/ar-es/compania/sala-de-prensa/news/nueva-droga-para-un-subtipo-de-cancer-de-pulmon.html.(acceded 24.09.2024).
47. Soemedi, R., et al., *Pathogenic variants that alter protein code often disrupt splicing.* Nat Genet, 2017. **49**(6): p. 848-855. https://doi.org/10.1038/ng.3837
48. Lu, J.J., et al., *Retrospective Analysis to Optimize the Detection of MET Exon 14 Skipping Mutations in Non-Small Cell Lung Cancer.* Diagnostics (Basel), 2024. **14**(11). https://doi.org/10.3390/diagnostics14111110
49. Pal, S.K., et al., *Characterization of Clinical Cases of Advanced Papillary Renal Cell Carcinoma via Comprehensive Genomic Profiling.* Eur Urol, 2018. **73**(1): p. 71-78. https://doi.org/10.1016/j.eururo.2017.05.033
50. Schmidt, L., et al., *Novel mutations of the MET proto-oncogene in papillary renal carcinomas.* Oncogene, 1999. **18**(14): p. 2343-50. https://doi.org/10.1038/sj.onc.1202547
51. Recondo, G., et al., *Molecular Mechanisms of Acquired Resistance to MET Tyrosine Kinase Inhibitors in Patients with MET Exon 14-Mutant NSCLC.* Clin Cancer Res, 2020. **26**(11): p. 2615-2625. https://doi.org/10.1158/1078-0432.CCR-19-3608
52. Yao, Y., et al., *Mutations in the MET tyrosine kinase domain and resistance to tyrosine kinase inhibitors in non-small-cell lung cancer.* Respir Res, 2023. **24**(1): p. 28. https://doi.org/10.1186/s12931-023-02329-1
53. Schoenfeld, A.J., et al., *Tumor Analyses Reveal Squamous Transformation and Off-Target Alterations As Early Resistance Mechanisms to First-line Osimertinib in EGFR-Mutant Lung Cancer.* Clin Cancer Res, 2020. **26**(11): p. 2654-2663. https://doi.org/10.1158/1078-0432.CCR-19-3563
54. Sequist, L.V., et al., *Osimertinib plus savolitinib in patients with EGFR mutation-positive, MET-amplified, non-small-cell lung cancer after progression on EGFR tyrosine kinase inhibitors: interim results from a multicentre, open-label, phase 1b study.* Lancet Oncol, 2020. **21**(3): p. 373-386. https://doi.org/10.1016/S1470-2045(19)30785-5
55. Hartmaier, R.J., et al., *Osimertinib + Savolitinib to Overcome Acquired MET-Mediated Resistance in Epidermal Growth Factor Receptor-Mutated, MET-Amplified Non-Small Cell Lung Cancer: TATTON.* Cancer Discov, 2023. **13**(1): p. 98-113. https://doi.org/10.1158/2159-8290.CD-22-0586.
56. Neklason, D.W., et al., *Activating mutation in MET oncogene in familial colorectal cancer.* BMC Cancer, 2011. **11**: p. 424. https://doi.org/10.1186/1471-2407-11-424
57. Tyner, J.W., et al., *MET receptor sequence variants R970C and T992I lack transforming capacity.* Cancer Res, 2010. **70**(15): p. 6233-7. https://doi.org/10.1158/0008-5472.CAN-10-0429
58. Chile, D.o.D.P.a.C.a.M.o.H.o. *Treatment recommendations*. 2018; Available from: https://diprece.minsal.cl/garantias-explicitas-en-salud-auge-o-ges/cancer-de-pulmon/recomendaciones/. (Acceded 24.09.2024).
59. Pecci, F., et al., *Activating point mutations in the MET kinase domain represent a unique molecular subset of lung cancer and other malignancies targetable with MET inhibitors.* Cancer Discov, 2024. https://doi.org/10.1158/2159-8290.CD-23-1217
60. van der Velden, D.L., et al., *The Drug Rediscovery protocol facilitates the expanded use of existing anticancer drugs.* Nature, 2019. **574**(7776): p. 127-131. https://doi.org/10.1038/s41586-019-1600-x

Preprints.org (www.preprints.org) | NOT PEER-REVIEWED | Posted: 6 November 2024 doi:10.20944/preprints202411.0367.v1

61. Wang, K., M. Li, and H. Hakonarson, *ANNOVAR: functional annotation of genetic variants from high-throughput sequencing data.* Nucleic Acids Res, 2010. **38**(16): p. e164. https://doi.org/10.1093/nar/gkq603.
62. Steinhaus, R., et al., *MutationTaster2021.* Nucleic Acids Res, 2021. **49**(W1): p. W446-W451.https://doi.org/10.1093/nar/gkab266
63. Jumper, J., et al., *Highly accurate protein structure prediction with AlphaFold.* Nature, 2021. **596**(7873): p. 583-589. https://doi.org/10.1038/s41586-021-03819-2
64. Gradler, U., et al., *Biophysical and structural characterization of the impacts of MET phosphorylation on tepotinib binding.* J Biol Chem, 2023. **299**(11): p. 105328. https://doi.org/10.1016/j.jbc.2023.105328

Disclaimer/Publisher's Note: The statements, opinions and data contained in all publications are solely those of the individual author(s) and contributor(s) and not of MDPI and/or the editor(s). MDPI and/or the editor(s) disclaim responsibility for any injury to people or property resulting from any ideas, methods, instructions or products referred to in the content.